THROUGH SKIN IMAGING for AIRCRAFT ASSEMBLY using PULSED - TRANSIENT THERMOGRAPHY

N.P. Avdelidis[1, 2], D.P. Almond[1]
[1] Materials Research Centre, University of Bath, Bath, UK; [2] IRT & Materials Consultancy, Volos, Greece.

Abstract: An investigation has been made of the potential of pulsed - transient thermography for identifying the location of fixtures beneath aircraft skins to facilitate accurate automated assembly operations. Experimental studies have been made of 1.6mm thick aluminium skins and both 2mm and 4mm thick carbon fibre reinforced plastic (CFRP) composite skins over both aluminium and composite struts, representing fixtures. For the thin CFRP case (i.e. 2mm skin), the strut behind the skin can be easily imaged and centre line location determined to an accuracy of 0.5mm. Greater difficulty is experienced in the thick CFRP (i.e. 4mm skin) and aluminium cases caused by, in the first case, the thickness of the skin material, and in the second instance, the sensitivity to the thermal contact resistance between the surfaces. For the aluminium case, modelling results show a thermal contact resistance between two high thermal conductivity surfaces to have far greater effect on thermal image degradation than between two lower thermal conductivity CFRP surfaces. A modest loading of such parts, however, reduces the effect of the thermal contact resistance and enables a sub-skin strut to be imaged and located to a similar accuracy to that achieved with the 2mm CFPR skin positioned over the CFRP strut.

Introduction: In the 1980's, Vavilov and Taylor [1] discussed the principles of active infrared thermographic non-destructive testing as a means of providing quantitative information about hidden defects or features in a material. Since then, numerous groups worldwide have used infrared investigation techniques in the inspection of subsurface defects and features, thermo-physical properties, coating thickness and hidden structures [2 - 4]. The capabilities of the technique for detecting and imaging subsurface defects have been greatly enhanced and the defect imaging process is now well understood [5, 6].
In this work, the objective was to study the ability of pulsed – transient thermography to locate anchoring points beneath the outer skin of aircraft structures, to facilitate automated drilling and fixing. Typical test structures, comprising of 1.6mm thick aluminium skins and both 2mm and 4mm thick carbon fibre reinforced plastic (CFRP) composite skins over both aluminium and composite struts respectively, were investigated experimentally and analysed using finite difference thermal modelling software, taking into consideration the size and depth of the features, as well as their thermal properties [7]. The ability of the technique to detect a subsurface fixing and to offer information about its location was investigated.

Experimental: The representative test structures (figure 1), comprising an Al aircraft skin (1.6mm) positioned over a thick Al strut and of CFRP skin (2mm or 4mm) over a thick CFRP strut, were analysed using the ThermoCalc-3D software. The dimensions of all investigated panels were 500 x 500 mm. The width of the strut was 100 mm. The size and depth of the features, as well as the thermal properties of the investigated materials were taken into account. Furthermore, the effect of thermal contact resistance (the air gap between skin and strut) was also considered. For this reason, the models were run using different values of air gap [7] such as 1, 10, 50 and 100 μm, as well as with having the perfect contact between the two surfaces (zero air

gap). The thermal and physical properties of the materials that were used during modelling are shown in table 1, whilst the heating time parameters shown in table 2 were used for the models.

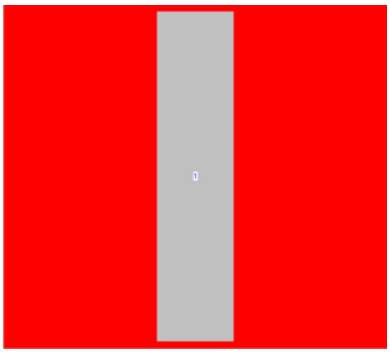

Figure 1: Rear view of modelled structures

Material	k ($Wm^{-1}K^{-1}$)	Cp ($JKg^{-1}K^{-1}$)	ρ (Kgm^{-3})
Al 2024-T3	126	961	2768
CFRP (⊥ fibre)	0.8	1200	1600
CFRP (| | fibre)	7	1200	1600
Air	0.026	1007	1.16

Table 1: Properties used during modelling

Test Structure	Heat Time (s)	End Time (s)	Time Step (s)
Al Skin of 1.6mm Over Al Strut	0.003	0.5	0.003
CFRP Skin of 2mm Over CFRP Strut	0.003	5	0.05
CFRP Skin of 4mm Over CFRP Strut	0.003	20	0.2

Table 2: Heating time parameters used during modelling

For the experimental work, an integrated pulsed thermographic system (Thermoscope) employing a medium wave infrared camera (Merlin 3-5 μm by Indigo) was utilised. The non-destructive evaluation system has an integrated flash heating system with a power output of 2KJ in 2 to 5 ms. The infrared camera uses a cooled indium antimonide detector with a frame rate of 60 Hz and a focal plane array pixel format of 320 (H) x 256 (V). Three panels, a 1.6mm thick Al (2024-T3) alloy skin over an Al strut, a 2mm thick CFRP skin over a CFRP strut and a 4mm thick CFRP skin over CFRP strut, were examined during this research work (similar to thermal modelling). The contrast of the thermal images of the subsurface fixtures in relation to time was measured (plots of contrast –vs.- time). Information concerning the centre line of the struts was obtained from the thermal images (a line was marked on the skin surface to show the centre line of the strut).

In the Al case, since the thermal conductivity is exceptionally high, the maximum frame rate (59.88 frames per second) was used for the recording of the images. In order to avoid the high reflectance of Al during investigation and to record thermal images, the sample was painted with a water based black paint. Furthermore, in order to reduce the thermal contact resistance (air gap)

that it is formed between the two surfaces (skin and strut) it was necessary to apply a load between the panel and the strut. In the first instance, bending the strut to form a low curvature fixing and wrapping the skin over it achieved this (two bending positions of 2.5 cm and 5 cm were studied). In the second instance, the panel was examined at various loadings – pressures using the test rig shown in figure 2.

Figure 2: Test rig used to apply a load to a strut beneath a skin.

In contrast to the work on Al parts, it was found that the thin CFRP skin (i.e. 2mm) over the CFRP strut could be imaged satisfactorily without significant loading. In the case of the 4mm CFRP skin over the CFRP strut, the test rig was used in a similar way to the Al case. In addition, due to the relatively low thermal conductivity of the CFRP material the thermal images during the cooling down process were acquired with a frame rate of 7.49 frames per second (for the 2mm skin) and 3.75 frames per second (for the 4mm skin).
Furthermore, the systems and the pressures that were applied on the structures where the test rig was use, were:

Test Structure	Pressure - Loading					
	0.04	0.1	0.165	0.290	0.490	0.650
Al skin of 1.6mm over Al strut	Yes	Yes	Yes	Yes	Yes	Yes
CFRP skin of 4mm over CFRP strut	Yes	Yes	Yes	Yes	Yes	No

Table 3: Examined systems and loadings used during thermographic inspection

The dimensions of the 2mm and the 4mm CFRP skins, as well as the 1.6mm Al skin were 300 x 275 mm (width x length). The width of the CFRP strut was 62.4 mm and its thickness 5 mm, whilst in the case of the Al strut the width was 50.8 mm and its thickness 3.7 mm. The lay-up of the fibres in the CFRP material was: $[(\pm 45°, 0_2, 90_2°)_2]_2$.
Finally, in all cases, 5 line profiles along the X-axis at 20, 74, 128, 182 and 236 (Y pixel values) were taken in order to define the centre of the strut using the FWHM (Full Width Half Maximum) approach.

Results & Discussion: The following remarks can be made about the modelling results (figures 3-6):

- The peak contrast of 4mm CFRP skin over CFRP strut is 2 times smaller than that of 2mm CFRP skin over CFRP strut, whilst its time scale (thermal transient phase) is 4 times longer.
- The 4mm CFRP skin over the CFRP strut presents the lowest thermal contrast amongst the tested modelled structures, while its time scale (thermal transient phase) is the longest (i.e. 20 seconds).

It can also be seen that the peak contrast value of Al is approximately 4.65 times greater than that of the CFRP (2mm skin), for zero air gap, since the differences of the Peak ΔT values are 0.05028 K for the Al and 0.0108 K for the CFRP. In other words, CFRP and Al behave differently to a particular extend because of dissimilar thermal properties. The thermal properties of CFRP are closer to those of air, than are those of Al. Furthermore, the contrast for Al parts becomes much smaller than that for CFRP where thin air layers are present (figure 6). This is an indication of the sensitivity of the contrast to contact when the two surfaces are of a high thermal conductive material such as Al.

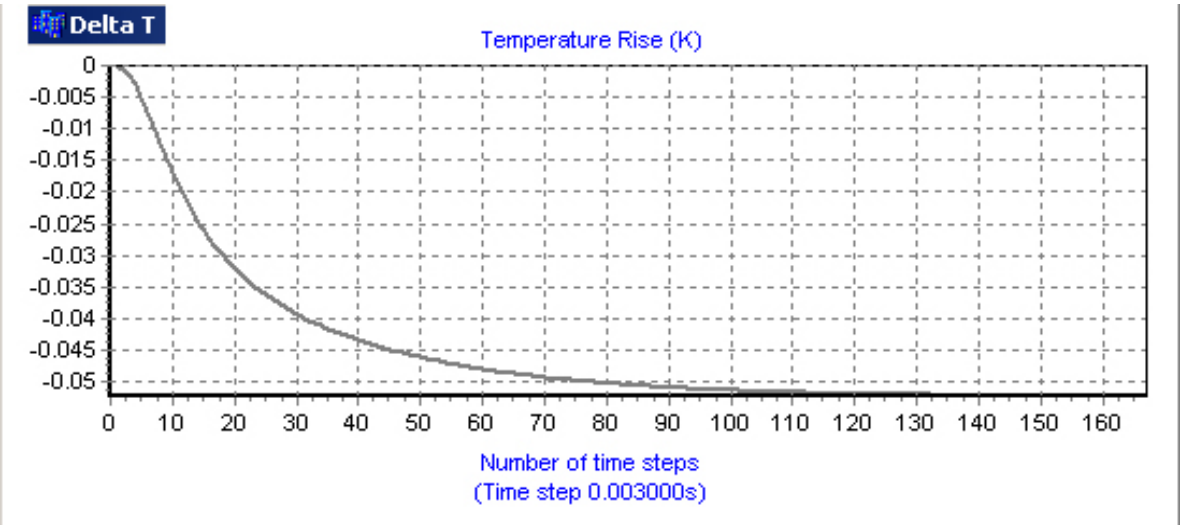

Figure 3: Modelling: thermal contrast vs. time plot of 1.6mm Al alloy skin over Al alloy strut.

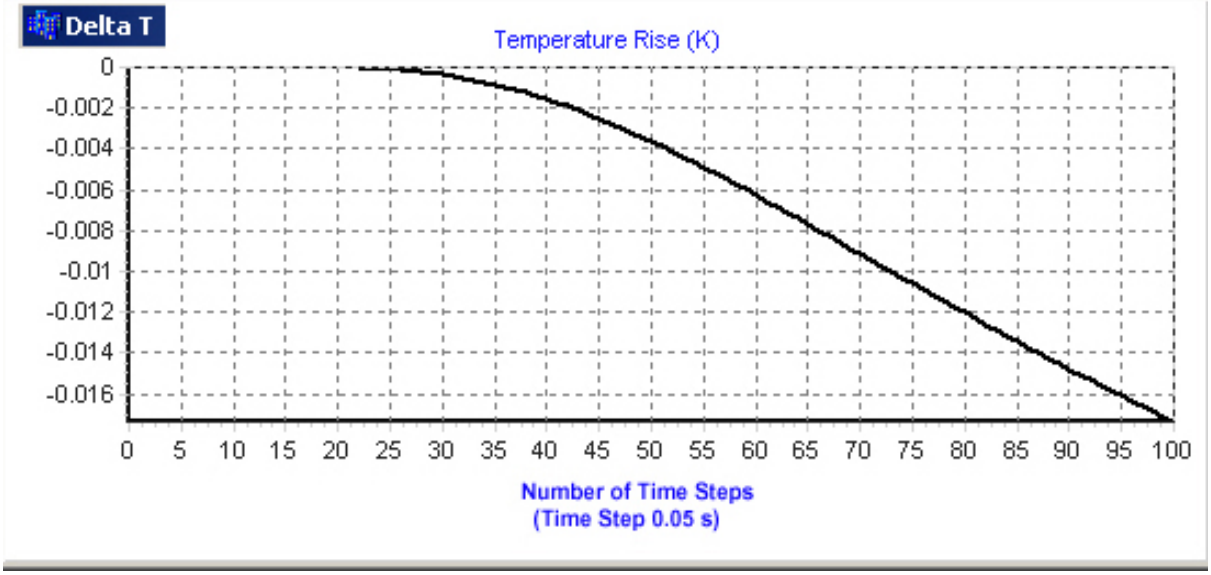

Figure 4: Modelling: thermal contrast vs. time plot of 2mm CFRP skin over CFRP strut

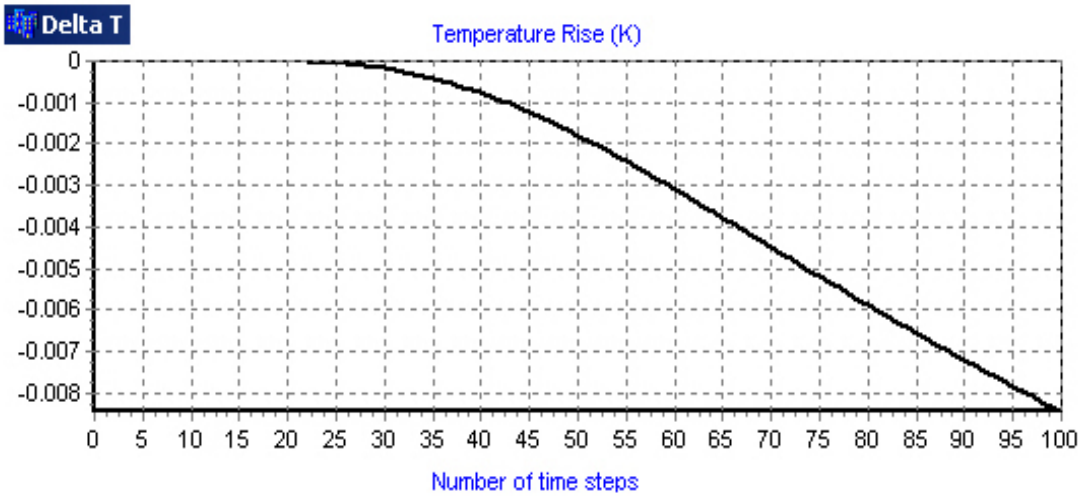

Figure 5: Modelling: thermal contrast vs. Time plot of 4mm CFRP skin over CFRP strut

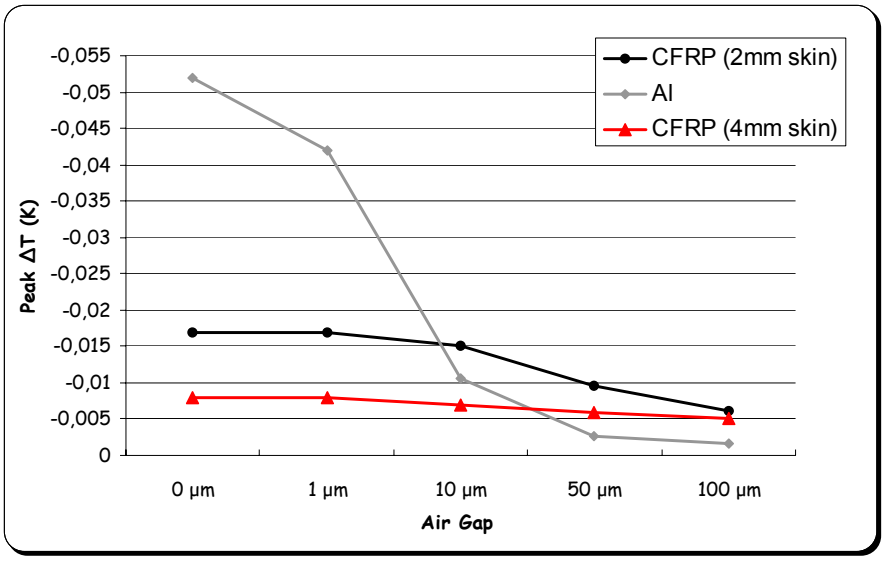

Figure 6: Modelling: peak ΔT against air gaps for CFRP and aluminium panels

Experimental results from the analysis of the Al panel are shown in figures 7 - 11. Since weak images were obtained using the raw thermal image for the two degrees of loading studied, synthetic 1st time derivative images were employed. In both loading situations, at early times (i.e. 0.1 seconds) the best results were obtained, i.e. centre line being within 1 pixel of the true centre line. However, at later transient times the variability is increased (up to 4 pixels in the 2.5 cm bending and up to 5.5 pixels in the 5 cm bending). Results obtained using the test rig with various pressures are shown in figures 9, 10 and 11. As previously, the 1st time derivative images were necessary in order to reveal the location of the strut. The images shown in figure 9 reveal the aluminium strut underneath the thin aluminium skin. Only the two edges of the strut form contrast minima because of the deformation of the skin. The pixel numbers of the two minima were determined from X-axis line profiles and the strut centre was then estimated to be mid-way between these two minima. Since the thermal contrast was found to be the highest in the case of maximum loading (i.e. 0.650kN), 5 line profiles along the X-axis at 20, 74, 128, 182 and 236 (Y pixel values) were acquired at various times only at that loading, in order to estimate the centre line of the strut during the transient phase of the thermographic data.

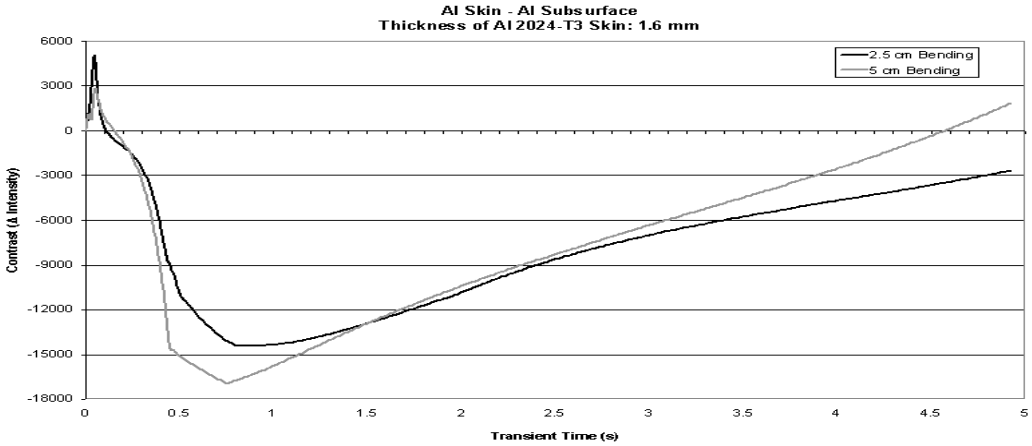

Figure 7: Thermal contrast curves of Al panel

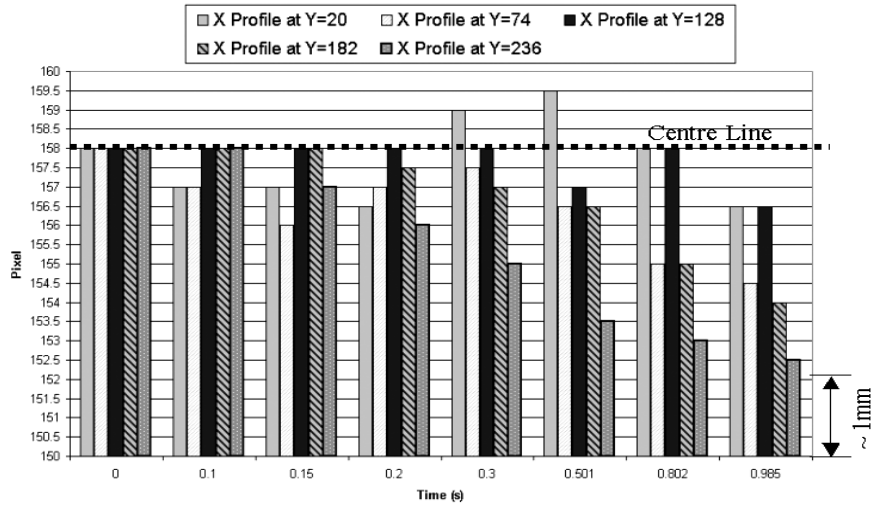

Figure 8: Pixel value of centre line of strut at positions along the length of the strut– vs.- Transient Time for Al panel in the 5cm bending condition.

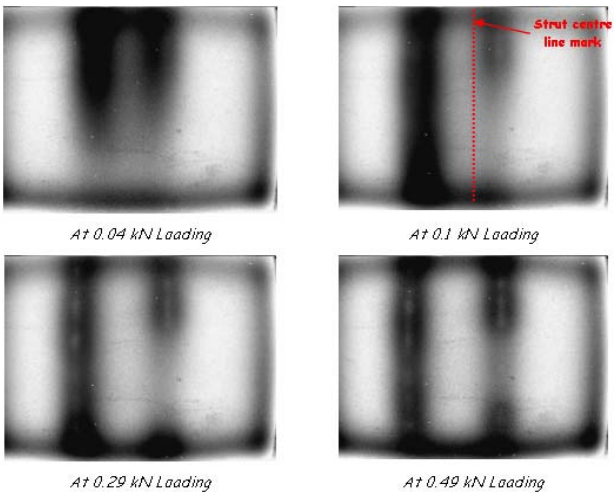

Figure 9: Thermal images for Al panel in the 5cm bending condition.

As far as the experimental results of CFRP are concerned, in the case of the thin CFRP structure (i.e. 2mm), it was found that the thermal images and the thermal contrast curve were very similar to the modelling simulations. The centre of the strut was then calculated from representative line profiles and it was found that at relatively early times (i.e. up to 5.344 seconds) the best results are accomplished (i.e. no variability) and with an overall satisfactory result; largest variability of 1 pixel or 0.465 mm (figure 10).

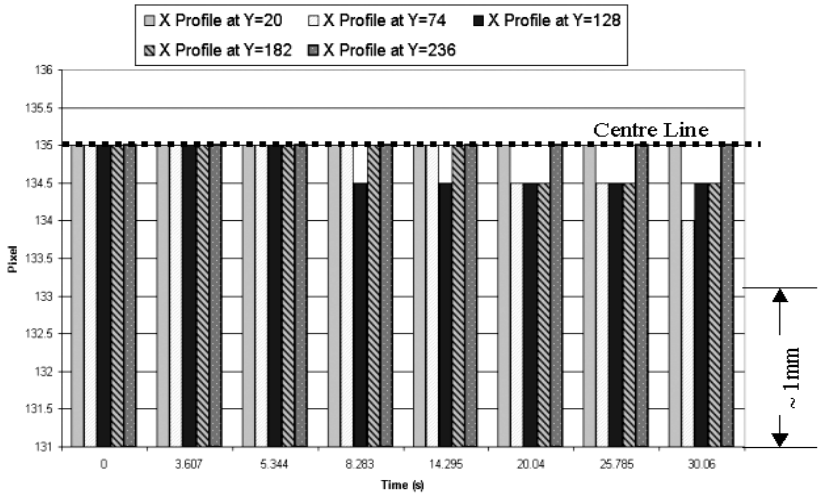

Figure 10: Pixel value of centre line of strut at positions along the length of the strut– vs.- transient time for 2mm thick CFRP skin and strut.

In the case of the 4mm CFRP skin over the CFRP strut, it was found that the 1st time derivative presentation of thermographic data was necessary to show the location of the strut. The images shown in figure 11 reveal the strut underneath the thick composite skin. The pixel numbers of the two half minimum signal points were determined from X-axis line profiles and the strut centre was then estimated to be mid-way between these two points. Since the thermal contrast was found to be the highest in the case of maximum loading (i.e. 0.490kN), X-axis line profiles were acquired at various times only at that loading, in order to estimate the centre line of the strut during the transient phase of the thermographic data.

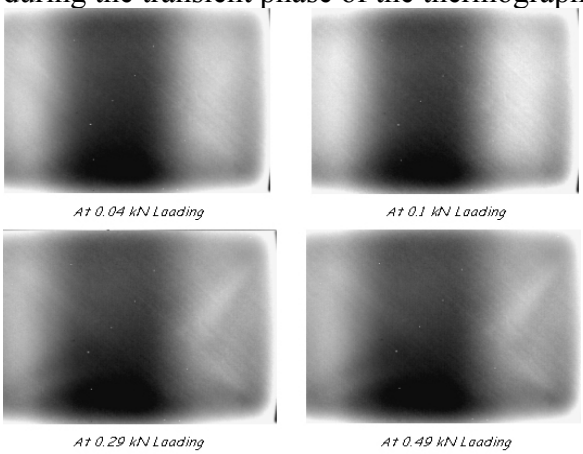

Figure 11: Thermal images acquired at maximum contrast & at different loads for 4mm CFRP skin and strut.

In the tested structure of 4mm CFRP skin over CFRP strut, as the thermal conductivity is relatively low, the thermal transient phase is fairly long. 5 line profiles along the X-axis were taken and the variability of the pixel value estimated to define the centre of the strut is shown in figure 12. It can also be seen that at relatively early times (up to 6.4 seconds) the best results are accomplished, since at these times there is very little variability.

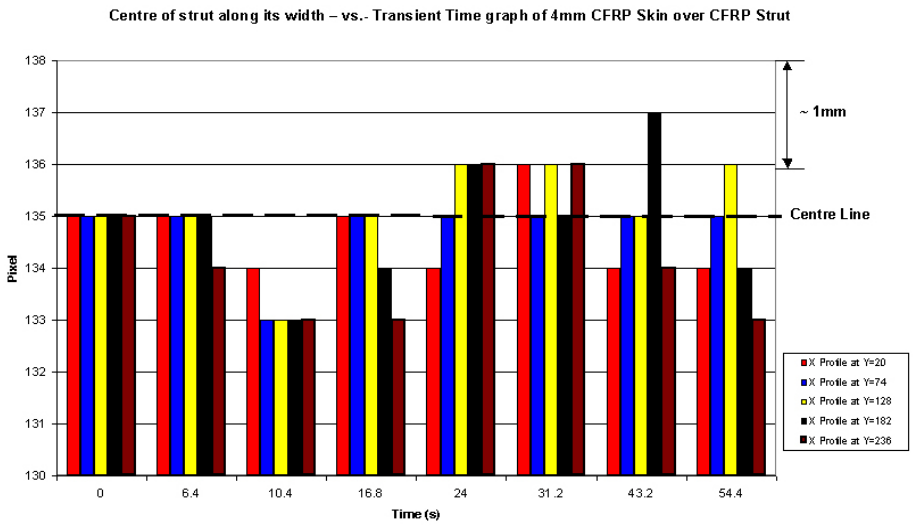

Figure 12: Pixel value of centre line of strut at positions along the length of the strut– vs.- transient time for 4mm thick CFRP skin and strut.

Conclusions: In the assembly of large non-rigid structures there is a need to locate with certainty fastening points and to monitor sealant distribution and other types of contact beneath outer skins. Transient - pulsed thermography has emerged in recent years as a means of "seeing" through skins [8, 9]. The technique has been demonstrated to work well for CFRP and Al alloy skins. The results of this work indicate that transient thermography can be used effectively for the detection of subsurface features located beneath composite and Al alloy skins. It shows great potential as far as locating the centre of a fixing accurately. The accuracy of the location of centre lines of subsurface struts for both the Al and the CFRP cases was better than 0.5 mm.

Acknowledgements: Work funded by the EU (Growth Programme G1RD-CT-2001-00673 - AHEAD). The authors would also like to thank Airbus for providing the Al alloy skin.

References:

1. V.P. Vavilov, R. Taylor, Theoretical and practical aspects of the thermal NDT of bonded structures', Research Techniques in NDT, Academic Press, Vol 5, pp. 239-280, 1982.
2. X. Maldague, F. Galmiche, A. Ziadi, Advances in pulsed phase thermography, Journal of Infrared Physics & Technology, 43(3-5), pp. 175-181, 2002.
3. N.P. Avdelidis, B.C. Hawtin, D.P. Almond, Transient thermography in the assessment of defects of aircraft composites, Journal of NDT & E International, 36(6), pp. 433-439, 2003.
4. T. Sakagami, S. Kubo, Applications of pulse heating thermography and lock-in thermography to quantitative nondestructive evaluations, Journal of Infrared Physics & Technology, 43(3-5), pp. 211-218, 2002.
5. S.M. Shepard, Advances in pulsed thermography, SPIE Proceedings Thermosense XXIII, Vol 4360, pp. 511-515, 2001.
6. N. Ludwig, P. Teruzzi, Heat losses and 3D diffusion phenomena for defect sizing procedures in video pulse thermography, Journal of Infrared Physics & Technology, 43(3-5), pp. 297-301, 2002.

7. N.P. Avdelidis, D.P. Almond, Transient thermography as a through skin imaging technique for aircraft assembly: modelling and experimental results, Journal of Infrared Physics & Technology, 45(2), pp. 103-114, 2004.
8. N.P. Avdelidis, D.P. Almond, Transient thermography as a through skin imaging technique for aircraft assembly, Journal of Insight, 46(4), pp. 200-202, 2004.
9. N.P. Avdelidis, D.P. Almond, Through skin sensing assessment of aircraft structures using pulsed thermography, Journal of NDT & E International, 37(5), pp. 353-359, 2004.